

A Bayesian model predicts the response of axons to molecular gradients

Duncan Mortimer^{a,1}, Julia Feldner^{a,b,1}, Timothy Vaughan^{a,1}, Irina Vetter^a, Zac Pujic^a, William J. Rosoff^a, Kevin Burrage^{b,c}, Peter Dayan^d, Linda J. Richards^{a,e}, and Geoffrey J. Goodhill^{a,f,2}

^aQueensland Brain Institute, ^bInstitute for Molecular Bioscience, ^cSchool of Biomedical Sciences, and ^fSchool of Mathematics and Physics, The University of Queensland, St. Lucia, QLD 4072, Australia; ^eComputing Laboratory, University of Oxford, Oxford OX1 3QD, United Kingdom; and ^dGatsby Computational Neuroscience Unit, University College London, London WC1E 6, United Kingdom

Edited by Charles F. Stevens, The Salk Institute for Biological Studies, La Jolla, CA, and approved May 6, 2009 (received for review February 5, 2009)

Axon guidance by molecular gradients plays a crucial role in wiring up the nervous system. However, the mechanisms axons use to detect gradients are largely unknown. We first develop a Bayesian “ideal observer” analysis of gradient detection by axons, based on the hypothesis that a principal constraint on gradient detection is intrinsic receptor binding noise. Second, from this model, we derive an equation predicting how the degree of response of an axon to a gradient should vary with gradient steepness and absolute concentration. Third, we confirm this prediction quantitatively by performing the first systematic experimental analysis of how axonal response varies with both these quantities. These experiments demonstrate a degree of sensitivity much higher than previously reported for any chemotacting system. Together, these results reveal both the quantitative constraints that must be satisfied for effective axonal guidance and the computational principles that may be used by the underlying signal transduction pathways, and allow predictions for the degree of response of axons to gradients in a wide variety of in vivo and in vitro settings.

axon guidance | chemotaxis | growth cone | nerve growth factor | nerve regeneration

Endogenous chemical gradients are a key source of information used by developing axons when wiring up the nervous system. Furthermore, artificially generated gradients are a potential therapy for restoring connectivity after neural injury. Many of the molecular gradients that direct axons in the developing nervous system have recently been identified, together with some of the signaling pathways through which they operate (1–8). However, our understanding of the mechanisms by which axons actually detect gradients remains qualitative. This limits our ability to predict both the response of axons when gradients are perturbed and the optimal parameters for promoting regrowth after injury.

To be guided by a gradient, axons must be able to detect small spatial variations in receptor binding. This requires integrating signals from spatially distributed receptors to make a decision as to the direction of the gradient. Resources within the growth cone can then be marshaled appropriately by this information, for instance, via the production of steep gradients of intracellular signaling molecules (8). Although there is evidence for a role for gradients of molecules such as Ca^{2+} in this latter step (9, 10), very little is known about the computations required to accurately make the initial decision.

What constrains the ability of an axon to make a decision regarding gradient direction? Both experimental and computational work addressing chemotaxis in related systems such as bacteria, leukocytes, and *Dictyostelium* has identified the fundamental role of noise in limiting gradient perception. Noise can arise from low numbers of ligand molecules, from the stochastic nature of receptor binding, and from intracellular signaling pathways (11–16). Such constraints must also apply to axonal gradient sensing (17, 18), but the implications of this for under-

standing axonal responses both in vivo and in vitro have not been systematically explored.

Noise in gradient sensing is a form of uncertainty in sensory information processing. In recent years, a “normative” (usually Bayesian) approach has proved to be a powerful technique for understanding how biological nervous systems deal with sensory uncertainty (19–22). This approach dissects the computational logic of complex behaviors by comparing actual, observed performance with the best performance possible given the information that is available to this system. However, barring a few exceptions (e.g., refs. 23, 24, and 25), such an approach has been applied predominantly at the systems, rather than molecular, level.

In the first part of this article, we develop a Bayesian model for the optimal determination of gradient direction based on combining measurements from noisy, spatially distributed receptors. This model allows us to predict analytically the proportion of correct decisions an axon should make about gradient direction as a function of gradient steepness and absolute concentration. In the second part of this article, we directly test this prediction. In particular, we perform the first large-scale experimental investigation of the dependence of the response of rat early postnatal dorsal root ganglion (DRG) axons on the steepness and concentration of gradients of nerve growth factor (NGF). We examine the strength of response of DRG axons for 4 different NGF gradient steepnesses, each over several orders of magnitude of NGF concentration (38 different combinations of steepness and concentration in total), by using an assay we recently introduced that allows precise control over these parameters (26, 27). This provides by far the largest dataset yet presented for how axonal response to gradients varies with gradient parameters. Remarkably, these data fit well with our Bayesian model, thus directly validating our analytical prediction for chemotactic performance.

Results

Bayesian Model of Spatial Gradient Sensing. A fundamental constraint on the performance of any chemotaxing system is random fluctuations in the pattern of receptors that are bound at any instant (11, 16). This means that, even if there were no thermal noise in the number of ligand molecules available for binding, it is still possible that the instantaneous pattern of binding will not accurately reflect the external gradient conditions. It is therefore important to consider how, given this fundamental uncertainty, a chemotacting system such as an axon could best make a decision about gradient direction.

Author contributions: G.J.G., K.B., P.D., and L.J.R. designed research; D.M., J.F., T.V., I.V., Z.P., and W.J.R. performed research; T.V. contributed new reagents/analytic tools; J.F. and T.V. analyzed data; and D.M., J.F., T.V., and G.J.G. wrote the paper.

The authors declare no conflict of interest.

This article is a PNAS Direct Submission.

¹D.M., J.F., and T.V. contributed equally to this work.

²To whom correspondence should be addressed. E-mail: g.goodhill@uq.edu.au.

This article contains supporting information online at www.pnas.org/cgi/content/full/0900715106/DCSupplemental.

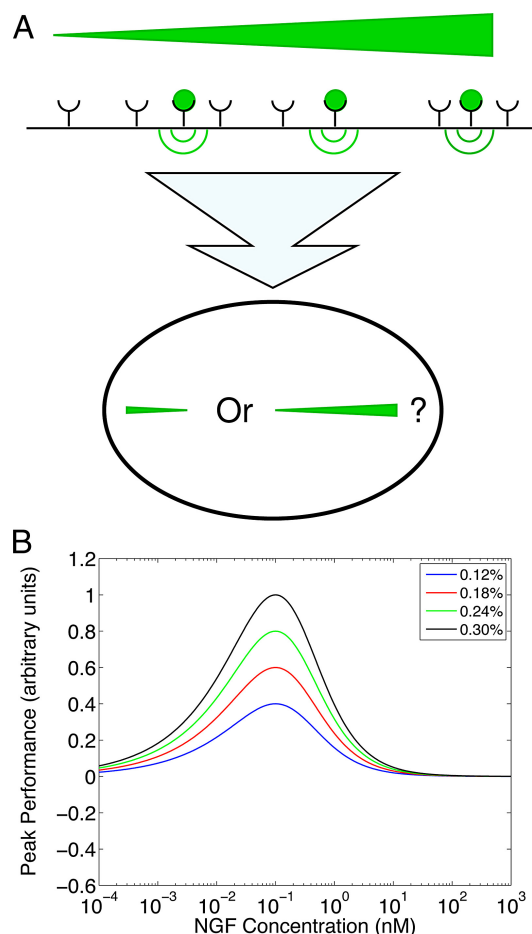


Fig. 1. Bayesian model of spatial gradient detection. (A) Model growth cone (for more detail see Fig. S1). Receptors on the surface bind ligand molecules probabilistically according to standard Michaelis–Menten kinetics. Signals from the bound receptors are then combined in the growth cone to optimally decide the most consistent gradient direction for that pattern of ligand binding. Although there are several intuitively obvious decision rules the growth cone could employ, determining the provably optimal strategy is nontrivial. We show that the optimal rule is to weight the signal from each bound receptor by its distance from the center of the growth cone (see *SI Text*). The sizes of the growth cones in the bubble represent the degree of belief of the growth cone in the 2 hypotheses for gradient direction based on that particular pattern of receptor binding. (B) Chemotactic sensitivity curves calculated analytically for the optimal decision rule for the gradient parameters used experimentally. The percentages refer to the fractional change in concentration across $10\ \mu\text{m}$. We set $K_D = 0.3\ \text{nM}$ based on the best fit between the model and the data (see Fig. 3).

Inspired by its success in other biological domains, we therefore developed a Bayesian “ideal observer” model (22) to determine the optimal strategy by which any gradient-sensing device can most reliably extract directional information from a set of intrinsically noisy receptors distributed across its spatial extent (Fig. 1A). The model is described in more detail in the [supporting information \(SI\) Text](#) and Fig. S1. Briefly, we considered a 1-dimensional growth cone* with N randomly distributed receptors, exposed to a ligand gradient such that μ is the relative change in concentration across its spatial extent, and γ is the concentration at the center of the growth cone

*For simplicity we phrase our discussion in terms of making comparisons across the extent of only the growth cone. However, our arguments are not affected by whether the comparison takes place over a longer spatial range, for instance including part of the axon shaft.

relative to K_D . We calculated the likelihood function giving the probability of each pattern of receptor binding in terms of μ and γ . Using Bayes’ theorem, we then inverted this function to give the posterior probability of μ given the pattern of binding, assuming that the prior probability for μ is symmetric and concentrated near zero. The gradient direction is then estimated by comparing the posterior probabilities that the gradient points in one direction versus the other.

There are many obvious possibilities for how to combine information from spatially distributed receptors to determine gradient direction, perhaps the simplest being to add up the total amount of receptor binding on one side of the growth cone and compare it with the total amount of receptor binding on other side. However, the use of the Bayesian approach allowed us to determine the optimal strategy, i.e., the one that gives the most reliable estimate of gradient direction. We found that this optimal strategy is to calculate the sum of the positions of bound receptors, i.e., weighted by their distances from the center of the growth cone. That is, receptor binding at the extremities of the growth cone contributes more weight to the decision than receptor binding near the center. In *Discussion*, we consider several possible biological implementations for this optimal computation.

Predicting Performance as Gradient Parameters Are Varied. Variations in receptor binding statistics over the spatial extent of the growth cone are determined by the gradient steepness and the absolute concentration. We therefore asked how the performance of our Bayes-optimal growth cone should vary with these parameters. Our readout of performance in the model is the probability that the growth cone estimates the direction of the gradient correctly for given gradient conditions. We were able to show analytically (see *SI Text*) that this proportion of correct decisions given steepness μ and concentration γ is

$$P_{\text{correct}}(\gamma, \mu) \approx \frac{1}{2} + \sqrt{\frac{N}{24\pi}} \mu \sqrt{\frac{\gamma}{(1 + \gamma)^3}}$$

Thus, the model predicts that axonal response should be determined by a scaling constant times $\mu\sqrt{\gamma/(1 + \gamma)^3}$. We refer to this quantity as the signal-to-noise ratio (SNR). This SNR is plotted against absolute concentration for the same gradient steepnesses we subsequently used experimentally (Fig. 1B), using the value of the dissociation constant K_D we determined as described below. Our analysis does not depend on how the decision regarding gradient direction influences growth cone behavior, which could be, for instance, a turn or a change in growth rate. In *SI Text*, we also discuss the relative performance of alternative strategies for weighting receptor binding measurements.

Experimental Analysis of the Dependence of Axonal Response on Gradient Conditions. Testing the above theoretical prediction for performance requires assaying the degree of response of axons to a range of different gradient steepnesses and concentrations. As a robust model system, we therefore examined the response of early postnatal rat DRG explants to gradients of NGF (28) after 2 days in collagen gels (see refs. 26, 29, and 30). Gradients were generated by using a more refined version of the technology described in ref. 26 (see *Materials and Methods* and *Movie S1*). In particular, by printing precisely controlled concentrations of ligand at precisely defined locations on the surface of a collagen gel, we created gradients in the gel for which, at particular positions, both the gradient steepness and absolute concentration remained relatively stable for periods of days (26, 27). We printed exponential gradients of ligand of steepnesses 0.12, 0.18, 0.24, and 0.30% per 10 micrometers, and for each steepness varied absolute concentration in steps of half \log_{10} units from ≈ 0.001

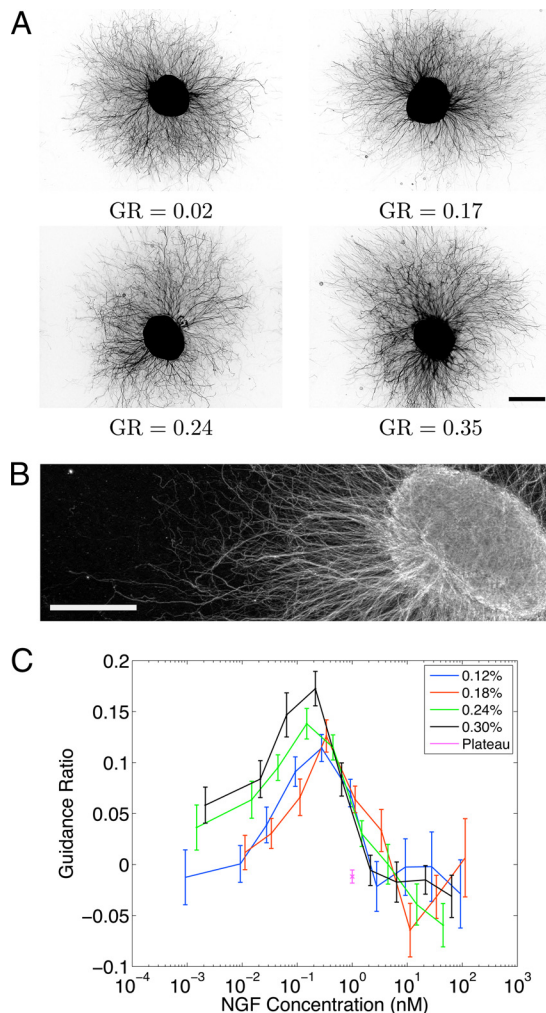


Fig. 2. Response of DRG explants to precisely controlled gradients of NGF. (A) Representative explants illustrating different guidance ratios (gradient is increasing upwards). (Scale bar, 400 μm .) (B) Higher-powered image of a typical subfield of neurites growing across the gradient (increasing upwards). (Scale bar, 250 μm .) (C) Explant asymmetry (guidance ratio) as a function of absolute concentration and gradient steepness (see *Methods*; n and values given in [Table S1](#)). Note that each curve peaked at approximately the same concentration, response dropped off faster at higher concentrations than lower concentrations, curve width increased with gradient steepness, and peak height tended to increase with steepness. Error bars are SEMs.

to 100 nM at the position in the gel at which explants were placed (see *SI Text* and [Fig. S2](#)). This resulted in 38 conditions in total with an average $n = 66$ explants per condition (for complete n values see [Table S1](#)). This is by far the most complete dataset of axonal responses to gradients yet measured.

[Fig. 2A](#) shows example explants displaying a range of different responses to the gradients. Asymmetry in neurite outgrowth from the explants was measured by using the “guidance ratio” (26), which compares the number of pixels representing neurites on the up-gradient versus the down-gradient side of the explant. Although simple, such a pixel-counting metric is fairly robust to image noise, and similar approaches have been used to quantify explant responses in related assays (e.g., [ref. 31](#)). [Fig. 2B](#) shows a higher-power image of a typical subfield of neurites. There is no obvious interaction between individual neurites, nor is there any obvious pattern of neurite turning. The latter suggests that the way the decision regarding gradient direction is read out by

these neurites may not be by turning but rather by, for instance, a change in growth rate depending on whether they are growing up or down the gradient. This issue remains to be addressed in more detail. [Fig. 2C](#) summarizes the guidance ratios of all explants as a function of gradient steepness and absolute concentration. For each steepness, the guidance ratio peaked at ≈ 0.3 nM NGF, and the height of the peak response tended to increase with gradient steepness ([Table S2](#)). Each peak was asymmetric (on a log scale), showing a more rapid decline in response for higher concentrations than for lower concentrations (see *SI Text*). Statistical comparisons of each condition with an NGF plateau control condition are given in [Table S1](#). Overall, it can be seen that responses vary systematically with gradient conditions and that this variation at least qualitatively resembles the variation predicted by the model ([Fig. 1B](#)). We return shortly to a more quantitative comparison with the theoretical model.

Trophic Versus Tropic Effects and Neurite Guidance Versus Neurite Initiation. It is conceivable that the explant asymmetry we observed in our gradients could be simply due to differential responses to absolute levels of NGF between the 2 sides of the explant rather than chemotactic guidance of axons by the gradient. However, several different lines of evidence discussed in *SI Text* support the argument that this is not the case (see also [Fig. S3](#)). It is also conceivable that the asymmetry in final outgrowth we observed could be due to an effect of the gradient on the direction of neurite initiation rather than guidance of neurites as they extend away from the cell body. We provided evidence that this was not an important effect by showing that the degree of guidance was not significantly degraded by printing the gradient up to 18 h after the explants were first embedded in the collagen (see *SI Text* and [Fig. S4](#)).

Axonal Response Shows Extreme Sensitivity. For the 0.24% and 0.3% gradients, measurable explant asymmetry was still present at an absolute concentration of ≈ 2 pM NGF. A 0.3% change over 10 μm at 2 pM corresponds to an absolute change of ≈ 1 molecule per millimeter per 1,000 μm^3 (approximately the volume of a growth cone), an astonishingly high level of sensitivity. These results reduce by 2 orders of magnitude a previous estimate (26) for the minimum concentration change across a growth cone that (when averaged over 2 days for a large number of axons) produces a measurable chemotactic response. This far exceeds the chemotactic sensitivity so far measured for any other biological or physical device.

The surprising nature of these results can be illustrated by some simple calculations. Consider for instance a simplified growth cone of width 10 μm , with 1,000 receptors on one side and 1,000 on the other, growing in a gradient of slope 0.3% at three absolute concentrations: 0.003, 1, and 3 nM. Using our estimated K_D of 0.3 nM, at a concentration of 0.003 nM, we have $\gamma = C/K_D \approx 0.01$ on the down-gradient side and $\gamma \approx 0.01003$ on the up-gradient side. The probability that each receptor is bound is $\gamma/(1 + \gamma)$, giving an expected number of bound receptors of 9.90 on the down-gradient side versus 9.93 on the up-gradient side at each instant (where fluctuating bound and unbound receptor states are assumed to be averaged over time to produce a meaningful signal). In this case, we observed a guidance ratio of ≈ 0.05 . We observed almost the same guidance ratio at a concentration of 1 nM, in which case $\gamma \approx 3$ on the down-gradient side and ≈ 3.01 on the up-gradient side. The comparison is now between ≈ 750 receptors and ≈ 750.6 bound receptors. In contrast, at a concentration of 3 nM we have $\gamma \approx 10$, and now the comparison is between 909.1 and 909.3 bound receptors. In this case, no statistically significant guidance response was seen, despite the similarity in the difference number of bound recep-

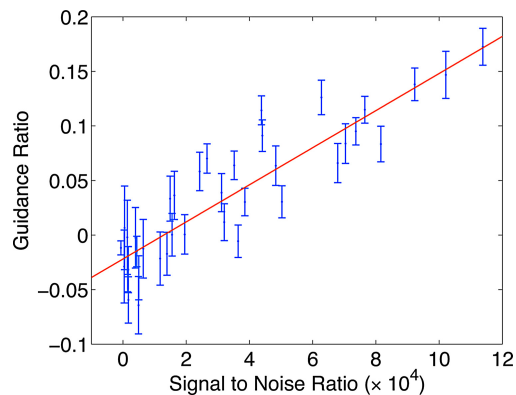


Fig. 3. Match between model and data. Measured guidance ratio plotted against the signal-to-noise formula predicted by the model. Error bars are SEMs. The red line is a linear fit (Pearson's $r = 0.90$). For the dependence of the fit on K_D see Fig. S5B

tors with the previous example. This illustrates that the observed response depends nontrivially on concentration and gradient steepness.

Experimental Data Are Predicted by the Bayesian Model. The above calculations make it clear that the axonal response depends in a nontrivial way on the gradient conditions. But is this quantitatively the dependence predicted by the Bayesian model? It is not possible to predict the absolute level of asymmetry observed in our experimental explants, because this depends on many unknown biological details of how axons convert decisions about gradient direction into directed motion. Rather, we can compare the way the response varies with gradient parameters between the model and the experiments. To do this quantitatively we plotted the SNR value predicted by the model against the experimentally measured guidance ratio for each of the 38 conditions in our experiment (Fig. 3). It can be seen that there is a remarkably strong correlation between the 2 sets of values (Pearson's $r = 0.90$). The only free parameter in this fit is the dissociation constant K_D . The K_D that maximized the correlation between the predicted SNR and the guidance ratio was 0.3 nM, which agrees well with the positions of the peaks in the guidance and outgrowth curves of Fig. 2 and Fig. S3A (the dependence of the correlation on K_D is shown in Fig. S5B).

Discussion

Comparison with Data from Conventional Collagen Assays. Our experimental data offer the first complete quantitative analysis of the behavior of axonal growth cones in molecular gradients and reveal sensitivity substantially more extreme than previously reported (26). The response of explants to gradients has been one of the key methods driving the field of axon guidance (5). However, this is usually in the context of the more conventional collagen gel coculture assay (31–34), where the gradient parameters are unknown and uncontrolled. Conventional collagen assays also suffer from variations between dishes in variables such as target size and thus the amount of factor released, separation between the explant and the ligand source, and transfection efficiency, all of which affect the molecular gradient experienced by the growth cones (35, 36). In contrast, in our more controlled assay we have shown that measurably different degrees of outgrowth asymmetry can be observed for remarkably subtle changes in gradient parameters. These variations may help explain some of the variability in the responses seen in conventional collagen assays.

Fitting the Model to the Data. Our ideal-observer model reproduces the overall variation in axonal behavior with gradient parameters by fitting only one parameter, the receptor-ligand dissociation constant K_D . The chemotropic response of growth cones to NGF is mediated by TrkA and p75. Although it was previously thought that both high- and low-affinity binding sites exist for NGF binding to TrkA/p75 (37), recent Scatchard analysis suggests that there is only 1 binding site with $K_D = 0.9 \pm 0.3$ nM (38). This is consistent with our determination of a similar value for K_D by using quite different methods.

It is remarkable that our data can be fit so well with a model that only considers the noise in the instantaneous receptor binding pattern. Noise inherent in thermal fluctuations in ligand numbers and in intracellular signaling pathways would be expected to provide additional constraints on performance, although potentially offset by temporal averaging of receptor binding measurements (11–15, 39). However, although reality is undoubtedly more complex than the situation represented in our model, this does not undermine the usefulness of our closed-form solution as a predictive tool for axonal responses.

Quantitative Implications. These calculations illustrate clearly that the level of response depends not on the absolute difference in receptor binding levels but on a nontrivial combination of gradient steepness and absolute concentration. We have been able to quantitatively capture this relationship from first principles in a simple analytical formula. Once more quantitative data becomes available for the gradients existing in vivo, it will be possible to use this equation to make precise predictions for how the fidelity of guidance should vary along a pathway, and to what degree perturbations in the gradient should affect guidance. Our equation can also be used to make quantitative estimates for how guidance should vary with parameters such as space, time, and rate of chemotropic factor production in in vivo situations and more conventional collagen gel coculture assays (35, 36).

Clearly the differences in average binding calculated above would need to be amplified by downstream processes to produce a response. This might involve, for instance, movement of receptors toward the up-gradient side (40). However, such amplification is only useful once the direction of the gradient has actually been detected and so is not a reliable mechanism for the detection itself. It is possible that the comparison may be occurring over a longer distance than the width of an individual growth cone, for instance, by taking into account information from receptors on the axon shaft. However, although this would change the details of the numbers calculated above, it would not change the optimal strategy we have determined for comparing information from spatially distributed receptors or its quantitative fit to the measured responses (due to the unknown scaling constant). It is also possible that, by internalizing bound NGF, the local gradient conditions are perturbed by each growth cone. However, for this to have an impact on our overall conclusions, it would be necessary for the perturbations to somehow amplify the SNR. Analogously to the remarks above regarding amplification by receptor redistribution, amplification by differential NGF uptake presupposes that the direction of the gradient has already been correctly determined.

Asymmetry with Concentration in the Guidance Response. Our model also offers a simple explanation for the asymmetry in chemotactic sensitivity seen in Fig. 2B. We assume that the growth cone has knowledge of the gradient only through the signals produced by its bound receptors. However, because of stochastic fluctuations in receptor density across the width of the growth cone, it will inevitably be the case for shallow gradients that occasionally, the receptor density fluctuations will be large enough to

dominate the true gradient signal. For the case of low ligand concentrations, few receptors are bound, and the size of this effect is small. However, as the ligand concentration increases the proportion of bound receptors increases, and thus the bias in the downstream signal due to nonuniform receptor density also increases, reducing the accuracy of decision making.

Possible Implementations of the Optimal Chemotaxis Strategy. We have shown that the optimal strategy is to calculate the sum of the positions of bound receptors weighted by their distances from the center of the growth cone. It is useful to think of this weighted sum as the difference in signal strength between the 2 sides of the growth cone. Implementing the optimal strategy then involves 2 steps: correctly weighting the inputs from the receptors so that receptors contribute in proportion to their distance from the center and then deciding whether the resulting signal is stronger on one side or the other. One possibility for how the growth cone might achieve the weighting step is by maintaining an inhomogeneous distribution of receptor-coupled effector proteins, with effector concentration proportional to the distance from the center of the growth cone. Peripheral receptors would then be presented with a greater number of effectors than central receptors, thus contributing more to the signal strength. Although direct evidence for or against this does not exist in growth cones, in *Dictyostelium* the most obvious candidate molecules for this role—various forms of G proteins—are known to be uniformly distributed across the leading edge (41), arguing against this possibility. Alternatively, the growth cone might preferentially distribute its receptors to the extremities, i.e., to the tips of filopodia. Some classes of guidance cue receptor have been observed to redistribute in the presence of a gradient—for example, on stimulation by a GABA gradient, GABA receptors cluster on the up-gradient side of rat spinal neuron growth cones, before a noticeable response occurs (40).

However, the analysis of the dynamical model of gradient detection of Skupsky et al. (42, 43) motivates a third alternative based on the properties of intracellular reaction diffusion pattern formation process triggered by receptor binding events. In the model presented in ref. 43, polarized cells are most sensitive to local environmental perturbations in concentration, which impinge at an angle of $\approx 60^\circ$ to the axis of polarization. This naturally awards peripheral receptors greater influence than those closer to the polarization axis. Although these authors focused on eukaryotic cell chemotaxis, similarities with the signaling networks underlying growth cone chemotaxis suggests that their results may also be relevant for growth cones (8, 44). The decision process itself, i.e., choosing the side on which the weighted signal is greatest, could then be implemented through adaptation and positive feedback, tuned to the appropriate length scale (8).

As discussed in the *SI Text*, some approximations to the Bayesian strategy have a lower absolute level of performance, but still produce a similar variation in performance with gradient parameters (see Fig. S6). Thus, it may be possible to achieve close to optimal performance by strategies that make less implementation demands on the growth cone than the optimal strategy. To directly measure implementation strategies would require a far more detailed analysis than has yet been performed experimentally of the spatiotemporal variations in distributions of signaling molecules inside growth cones exposed to gradients.

Conclusions

Ultimately, the quantitative predictions offered by our model allow a more precise understanding of in vivo events during both normal and abnormal nervous system development, and may facilitate the design of gradients that optimize the ability of the

nervous system to rewire itself after injury. Overall, these results suggest that optimality principles already demonstrated to be effective at the systems level will also be useful for understanding sensory information processing at the cellular level and point to directions for the quantitative understanding of nervous system development.

Materials and Methods

Tissue Preparation. DRGs were removed from the thoracic and lumbar regions of postnatal day P0–P3 rat pups, trimmed and stored in Hibernate E (phenol red; Brainbits) at 4 °C overnight. On the next day, the outer capsule was digested for 12 min in 0.25% trypsin/10 $\mu\text{g}/\text{mL}$ DNase1/ Ca^{2+} and Mg^{2+} free Hanks's balanced salt solution. The explants were centrifuged and resuspended in Leibowitz's L-15 medium containing L-glutamine and 0.45% D(+)-glucose 3 times.

Dry Collagen Gels. A 0.2% collagen gel solution was prepared on ice by mixing rat tail type I collagen stock solution (BD Biosciences) diluted with water to contain 0.2 mg/mL collagen, 27 μL of a 7.5% sodium bicarbonate solution per milliliter of original collagen stock, 1 \times OptiMEM (Gibco) and a mixture of 100 $\mu\text{g}/\text{mL}$ penicillin, 100 $\mu\text{g}/\text{mL}$ streptomycin, and 250 ng/mL amphotericin (Gibco). Collagen gels were prepared and 6 explants plated in a row in 35-mm tissue culture dishes as described previously (26).

Gradient Generation. Gradients of NGF (GroPep) were created by using a Nano-Plotter 2.0 (Gesim). The physical principles of gradient generation were as previously described (26, 27), but the precise details were different because of the greater flexibility of the Nano-Plotter compared with the technology used in ref. 26. Twelve stock solutions with exponentially increasing NGF concentration were “printed” onto the surface of the collagen gels in the form of 12 parallel lines 20 mm long and 1 mm apart, each line containing the same volume of stock (see Movie S1). Line 4 coincided with the position of the row of explants. The amount of NGF required in each line to produce the desired final concentration in the gel was calculated as previously described (26, 27). However, we also calculated correction factors for both the concentration and gradient steepness, to take into account the average gradient conditions existing over the complete time course of the experiment (see *SI Text* and Fig. S2). Four additional “pregradient” lines of only vehicle (0.1% BSA/PBS) were applied adjacent to the low-concentration side of the gradient (line 1) to avoid a possibly confounding gradient of collagen density near to the explants. After printing, dishes were returned to a 37 °C incubator with 5% CO_2 for a total explant incubation time of 40–48 h. Our standard control was to print a “plateau” by using the same methods, except with no change in NGF concentration between the different stocks. For delayed application of gradients (Table S3), DRG explants were embedded in collagen gel containing 0.1 nM NGF and a gradient resulting in 0.24% steepness with 0.3 nM NGF at the explant printed either immediately or after 2, 4, 8, 12, 18, or 24-h incubation at 37 °C.

Neurite Visualization. Explants embedded in collagen were fixed with an equal volume of 10% formaldehyde/0.1% Triton X-100 in PBS overnight. After 5 washes with PBS for 1 h each, explants were incubated overnight in 1 $\mu\text{g}/\text{mL}$ of the neuronal tubulin antibody TUJ1 (R&D Systems), followed by an additional 5 washes in PBS for 1 h each. The explants were then incubated overnight in the secondary antibody Alexa Fluor 488-conjugated goat anti-mouse IgG (1:1,000; Molecular Probes), washed 5 times in PBS for 1 h each, and photographed with an AxioCam HRm (Zeiss) camera on a Zeiss Imager Z1 fluorescence microscope.

Quantification of Explant Asymmetry and Total Outgrowth. By manually applying an appropriate intensity threshold to each image and discounting the region encompassing the explant tissue (using Adobe Photoshop), an estimate of the distribution of neurites in each image was obtained as in ref. 26. Outgrowth asymmetry was quantified by using the guidance ratio $\text{GR} = (\text{H} - \text{L})/(\text{H} + \text{L})$, H and L being the number of neurite pixels on the high and low ligand concentration sides of the explant, respectively.

ACKNOWLEDGMENTS. This work was supported by an Australian Postgraduate Award (to D.M.), an Australian Research Council Federation Fellowship (to K.B.), the Gatsby Charitable Foundation (P.D.), and Australian Research Council Discovery Grant DP0666126 and Australian National Health and Medical Research Council (Project Grant 456003, Senior Research Fellowship to L.J.R.).

1. Tessier-Lavigne M, Goodman CS (1996) The molecular biology of axon guidance. *Science* 274:1123–1133.
2. Song H, Poo M (2001) The cell biology of neuronal navigation. *Nat Cell Biol* 3:E81–E88.
3. Dickson BJ (2002) Molecular mechanisms of axon guidance. *Science* 298:1959–1964.
4. Huber AB, Kolodkin AL, Ginty DD, Cloutier JF (2003) Signaling at the growth cone: Ligand–receptor complexes and the control of axon growth and guidance. *Annu Rev Neurosci* 26:509–563.
5. Guan KL, Rao Y (2003) Signalling mechanisms mediating neuronal responses to guidance cues. *Nat Rev Neurosci* 4:941–956.
6. Plachez C, Richards LJ (2005) Mechanisms of axon guidance in the developing nervous system. *Curr Top Dev Biol* 69:267–346.
7. Zheng JQ, Poo MM (2007) Calcium signaling in neuronal motility. *Annu Rev Cell Dev Biol* 23:375–404.
8. Mortimer D, Fothergill T, Pujic Z, Richards LJ, Goodhill GJ (2008) Growth cone chemotaxis. *Trends Neurosci* 31:90–98.
9. Zheng JQ (2000) Turning of nerve growth cones induced by localized increases in intracellular calcium ions. *Nature* 403:89–93.
10. Hong K, Nishiyama M, Henley J, Tessier-Lavigne M, Poo M (2000) Calcium signalling in the guidance of nerve growth by netrin-1. *Nature* 403:93–98.
11. Berg HC, Purcell EM (1977) Physics of chemoreception. *Biophys J* 20:193–219.
12. Bialek W, Setayeshgar S (2005) Physical limits to biochemical signaling. *Proc Natl Acad Sci USA* 102:10040–10045.
13. Gregor T, Tank DW, Wieschaus EF, Bialek W (2007) Probing the limits to positional information. *Cell* 130:153–164.
14. van Haastert PJM, Postma M (2007) Biased random walk by stochastic fluctuations of chemoattractant–receptor interactions at the lower limit of detection. *Biophys J* 93:1787–1796.
15. Ueda M, Shibata T (2007) Stochastic signal processing and transduction in chemotactic response of eukaryotic cells. *Biophys J* 93:11–20.
16. Tranquillo RT (1990) in *Biology of the Chemotactic Response*, eds Armitage J, Lackie JM (Cambridge Univ Press, Cambridge, UK), pp 35–75.
17. Goodhill GJ, Urbach JS (1999) Theoretical analysis of gradient detection by growth cones. *J Neurobiol* 41:230–241.
18. Xu J, Rosoff WJ, Urbach JS, Goodhill GJ (2005) Adaptation is not required to explain the long-term response of axons to molecular gradients. *Development* 132:4545–4552.
19. Ernst MO, Banks MS (2002) Humans integrate visual and haptic information in a statistically optimal fashion. *Nature* 415:429–433.
20. Weiss Y, Simoncelli EP, Adelson EH (2002) Motion illusions as optimal percepts. *Nat Neurosci* 5:598–604.
21. Kording KP, Wolpert DM (2004) Bayesian integration in sensorimotor learning. *Nature* 427:244–247.
22. Kording K (2007) Decision theory: What “should” the nervous system do? *Science* 318:606–610.
23. Strong SP, Freedman B, Bialek W, Koberle R (1998) Adaptation and optimal chemotactic strategy for *E. coli*. *Phys Rev E* 57:4604–4617.
24. Libby E, Perkins TJ, Swain PS (2007) Noisy information processing through transcriptional regulation. *Proc Natl Acad Sci USA* 104:7151–7156.
25. Andrews BW, Iglesias PA (2007) An information-theoretic characterization of the optimal gradient sensing response of cells. *PLoS Comput Biol* 3:e153.
26. Rosoff WJ, et al. (2004) A new chemotaxis assay shows the extreme sensitivity of axons to molecular gradients. *Nat Neurosci* 7:678–682.
27. Rosoff WJ, McAllister R, Esrick MA, Goodhill GJ, Urbach JS (2005) Generating controlled molecular gradients in 3d gels. *Biotechnol Bioeng* 91:754–759.
28. Gundersen RW, Barrett JN (1979) Neuronal chemotaxis: Chick dorsal-root axons turn toward high concentrations of nerve growth factor. *Science* 206:1079–1080.
29. Letourneau PC (1978) Chemotactic response of nerve fiber elongation to nerve growth factor. *Dev Biol* 66:183–196.
30. Cao X, Shoichet MS (2003) Investigating the synergistic effect of combined neurotrophic factor concentration gradients to guide axonal growth. *Neuroscience* 122:381–389.
31. Caton A, et al. (2000) The branchial arches and hgf are growth-promoting and chemoattractant for cranial motor axons. *Development* 127:1751–1766.
32. Lumsden AG, Davies AM (1983) Earliest sensory nerve fibres are guided to peripheral targets by attractants other than nerve growth factor. *Nature* 306:786–788.
33. Tessier-Lavigne M, Placzek M, Lumsden AG, Dodd J, Jessell TM (1988) Chemotropic guidance of developing axons in the mammalian central nervous system. *Nature* 336:775–778.
34. Powell AW, Sassa T, Wu Y, Tessier-Lavigne M, Polleux F (2008) Topography of thalamic projections requires attractive and repulsive functions of netrin-1 in the ventral telencephalon. *PLoS Biol* 6:e116.
35. Goodhill GJ (1997) Diffusion in axon guidance. *Eur J Neurosci* 9:1414–1421.
36. Goodhill GJ (1998) Mathematical guidance for axons. *Trends Neurosci* 21:226–231.
37. Hempstead BL, Martin-Zanca D, Kaplan DR, Parada LF, Chao MV (1991) High-affinity ngf binding requires coexpression of the trk proto-oncogene and the low-affinity ngf receptor. *Nature* 350:678–683.
38. Wehrman T, et al. (2007) Structural and mechanistic insights into nerve growth factor interactions with the trka and p75 receptors. *Neuron* 53:25–38.
39. Rappel WJ, Levine H (2008) Receptor noise limitations on chemotactic sensing. *Proc Natl Acad Sci USA* 105:19270–19275.
40. Bouzigues C, Morel M, Triller A, Dahan M (2007) Asymmetric redistribution of gaba receptors during gaba gradient sensing by nerve growth cones analyzed by single quantum dot imaging. *Proc Natl Acad Sci USA* 104:11251–11256.
41. Jin T, Zhang N, Long Y, Parent CA, Devreotes PN (2000) Localization of the G protein betagamma complex in living cells during chemotaxis. *Science* 287:1034–1036.
42. Skupsky R, Losert W, Nossal RJ (2005) Distinguishing modes of eukaryotic gradient sensing. *Biophys J* 89:2806–2823.
43. Skupsky R, McCann C, Nossal R, Losert W (2007) Bias in the gradient-sensing response of chemotactic cells. *J Theor Biol* 247:242–258.
44. von Philipsborn AC, Bastmeyer M (2007) Mechanisms of gradient detection: A comparison of axon pathfinding with eukaryotic cell migration. *Int Rev Cytol* 263:1–62.